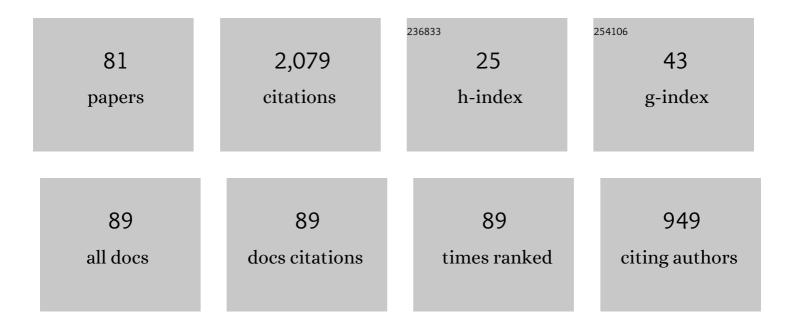
Christoph Englert

List of Publications by Year in descending order

Source: https://exaly.com/author-pdf/3422862/publications.pdf Version: 2024-02-01



CHDISTOPH ENCLEPT

#	Article	IF	CITATIONS
1	Exospheric Temperature Measured by NASAâ€GOLD Under Low Solar Activity: Comparison With Other Data Sets. Journal of Geophysical Research: Space Physics, 2022, 127, .	0.8	4
2	Examining the Wind Shear Theory of Sporadic E With ICON/MIGHTI Winds and COSMICâ€2 Radio Occultation Data. Geophysical Research Letters, 2022, 49, .	1.5	29
3	Vertical Coupling by Solar Semidiurnal Tides in the Thermosphere From ICON/MIGHTI Measurements. Journal of Geophysical Research: Space Physics, 2022, 127, .	0.8	16
4	Topside Plasma Flows in the Equatorial Ionosphere and Their Relationships to Fâ€Region Winds Near 250Âkm. Journal of Geophysical Research: Space Physics, 2022, 127, .	0.8	9
5	Intense Equatorial Electrojet and Counter Electrojet Caused by the 15 January 2022 Tonga Volcanic Eruption: Space―and Groundâ€Based Observations. Geophysical Research Letters, 2022, 49, .	1.5	27
6	Vertical Shears of Horizontal Winds in the Lower Thermosphere Observed by ICON. Geophysical Research Letters, 2022, 49, .	1.5	9
7	Validation of ICONâ€MIGHTI Thermospheric Wind Observations: 1. Nighttime Redâ€Line Groundâ€Based Fabryâ€Perot Interferometers. Journal of Geophysical Research: Space Physics, 2021, 126, e2020JA028726.	0.8	43
8	Determining the thermomechanical image shift for the MIGHTI instrument on the NASA-ICON satellite (Erratum). Optical Engineering, 2021, 60, .	0.5	0
9	Validation of ICONâ€MIGHTI Thermospheric Wind Observations: 2. Greenâ€Line Comparisons to Specular Meteor Radars. Journal of Geophysical Research: Space Physics, 2021, 126, e2020JA028947.	0.8	45
10	Atmosphereâ€lonosphere (Aâ€l) Coupling as Viewed by ICON: Dayâ€toâ€Day Variability Due to Planetary Wave (PW)â€Tide Interactions. Journal of Geophysical Research: Space Physics, 2021, 126, e2020JA028927.	0.8	14
11	Quasiâ€2â€Day Wave in Low‣atitude Atmospheric Winds as Viewed From the Ground and Space During January–March, 2020. Geophysical Research Letters, 2021, 48, e2021GL093466.	1.5	13
12	Temperature Tides Across the Midâ€Latitude Summer Turbopause Measured by a Sodium Lidar and MIGHTI/ICON. Journal of Geophysical Research D: Atmospheres, 2021, 126, e2021JD035321.	1.2	8
13	Evaluation of Atmospheric 3â€Đay Waves as a Source of Dayâ€ŧoâ€Đay Variation of the Ionospheric Longitudinal Structure. Geophysical Research Letters, 2021, 48, e2021GL094877.	1.5	9
14	Isolated Peak of Oxygen Ion Fraction in the Postâ€Noon Equatorial Fâ€Region: ICON and SAMI3/WACCMâ€X. Journal of Geophysical Research: Space Physics, 2021, 126, e2021JA029217.	0.8	5
15	First Results From the Retrieved Column O/N ₂ Ratio From the Ionospheric Connection Explorer (ICON): Evidence of the Impacts of Nonmigrating Tides. Journal of Geophysical Research: Space Physics, 2021, 126, e2021JA029575.	0.8	7
16	Q2DWâ€tide and â€ionosphere interactions as observed from ICON and groundâ€based radars. Journal of Geophysical Research: Space Physics, 2021, 126, e2021JA029961.	0.8	4
17	Comparison of ICON/MIGHTI and TIMED/TIDI Neutral Wind Measurements in the Lower Thermosphere. Journal of Geophysical Research: Space Physics, 2021, 126, e2021JA029904.	0.8	18
18	Regulation of ionospheric plasma velocities by thermospheric winds. Nature Geoscience, 2021, 14, 893-898.	5.4	25

#	Article	IF	CITATIONS
19	On-orbit Performance of the Thermospheric Wind and Temperature Instrument on the NASA ICON Mission. , 2021, , .		0
20	Laboratory demonstration of mini-MIGHTI: A prototype sensor for thermospheric red-line (630Ânm) neutral wind measurements from a 6U CubeSat. Journal of Atmospheric and Solar-Terrestrial Physics, 2020, 207, 105363.	0.6	6
21	Errors From Asymmetric Emission Rate in Spaceborne, Limb Sounding Doppler Interferometry: A Correction Algorithm With Application to ICON/MIGHTI. Earth and Space Science, 2020, 7, e2020EA001164.	1.1	11
22	Determining the thermomechanical image shift for the MIGHTI instrument on the NASA-ICON satellite. Optical Engineering, 2020, 59, 1.	0.5	5
23	Calibration lamp design, characterization, and implementation for the Michelson Interferometer for Global High-Resolution Thermospheric Imaging instrument on the Ionospheric Connection satellite. Optical Engineering, 2019, 58, 1.	0.5	5
24	On the uncertainties in determining fringe phase in Doppler asymmetric spatial heterodyne spectroscopy. Applied Optics, 2019, 58, 3613.	0.9	7
25	Retrieval of Lower Thermospheric Temperatures from O2 A Band Emission: The MIGHTI Experiment on ICON. Space Science Reviews, 2018, 214, 1.	3.7	26
26	The Ionospheric Connection Explorer Mission: Mission Goals and Design. Space Science Reviews, 2018, 214, 1.	3.7	152
27	Michelson Interferometer for Global High-Resolution Thermospheric Imaging (MIGHTI): Instrument Design and Calibration. Space Science Reviews, 2017, 212, 553-584.	3.7	116
28	Periodicities of polar mesospheric clouds inferred from a meteorological analysis and forecast system. Journal of Geophysical Research D: Atmospheres, 2017, 122, 4508-4527.	1.2	20
29	Michelson Interferometer for Global High-Resolution Thermospheric Imaging (MICHTI): Monolithic Interferometer Design and Test. Space Science Reviews, 2017, 212, 601-613.	3.7	40
30	The MIGHTI Wind Retrieval Algorithm: Description and Verification. Space Science Reviews, 2017, 212, 585-600.	3.7	74
31	High-efficiency echelle gratings for MICHTI, the spatial heterodyne interferometers for the ICON mission. Applied Optics, 2017, 56, 2090.	2.1	17
32	The As-Built Performance of the MIGHTI Interferometers. , 2016, , .		0
33	As-built Specifications of MIGHTI â \in The Thermospheric Wind and Temperature Instrument for the NASA ICON Mission. , 2016, , .		0
34	Spatial heterodyne spectroscopy at the Naval Research Laboratory. Applied Optics, 2015, 54, F158.	2.1	25
35	MIGHTI: The Spatial Heterodyne Instrument for Thermospheric Wind Measurements on Board the ICON Mission. , 2015, , .		5
36	Design and Laboratory Tests of the Michelson Interferometer for Global High-resolution		0

⁶⁶ Thermospheric Imaging (MIGHTI) on the Ionospheric Connection Explorer (ICON) Satellite. , 2015, , .

#	Article	IF	CITATIONS
37	High sensitivity trace gas sensor for planetary atmospheres: miniaturized Mars methane monitor. Journal of Applied Remote Sensing, 2014, 8, 083625.	0.6	4
38	Optical orbital debris spotter. Acta Astronautica, 2014, 104, 99-105.	1.7	25
39	Comparison of a photochemical model with observations of mesospheric hydroxyl and ozone. Journal of Geophysical Research D: Atmospheres, 2013, 118, 195-207.	1.2	15
40	Thermal sensitivity of DASH interferometers: the role of thermal effects during the calibration of an Echelle DASH interferometer. Applied Optics, 2013, 52, 8082.	0.9	13
41	Design of a real-fringe DASH interferometer for observations of thermospheric winds from a small satellite. , 2013, , .		2
42	The Michelson Interferometer for Global High-resolution Thermospheric Imaging (MIGHTI): Wind and Temperature Observations from the Ionospheric Connection Explorer (ICON). , 2013, , .		2
43	Measurement and modeling of the thermal behavior of a laboratory DASH interferometer. Proceedings of SPIE, 2012, , .	0.8	1
44	Bright polar mesospheric clouds formed by main engine exhaust from the space shuttle's final launch. Journal of Geophysical Research, 2012, 117, .	3.3	16
45	Low-cost, automated ground station for LEO mission support. IEEE Aerospace and Electronic Systems Magazine, 2011, 26, 12-18.	2.3	5
46	Compression Assembly of Spatial Heterodyne Spectroscopy Interferometers. Recent Patents on Space Technology, 2011, 1, 1-6.	0.1	0
47	Consequences of recent Southern Hemisphere winter variability on polar mesospheric clouds. Journal of Atmospheric and Solar-Terrestrial Physics, 2011, 73, 2013-2021.	0.6	34
48	Doppler Asymmetric Spatial Heterodyne (DASH) Interferometer from Flight Concept to Field Campaign. , 2011, , .		0
49	Laboratory and field tests of a Doppler Asymmetric Spatial Heterodyne (DASH) spectrometer for thermospheric wind observations. , 2011, , .		Ο
50	Tidally induced variations of polar mesospheric cloud altitudes and ice water content using a data assimilation system. Journal of Geophysical Research, 2010, 115, .	3.3	45
51	Spatial Heterodyne Imager for Mesospheric Radicals on STPSatâ€1. Journal of Geophysical Research, 2010, 115, .	3.3	41
52	Design and laboratory tests of a Doppler Asymmetric Spatial Heterodyne (DASH) interferometer for upper atmospheric wind and temperature observations. Optics Express, 2010, 18, 26430.	1.7	48
53	Initial ground-based thermospheric wind measurements using Doppler asymmetric spatial heterodyne spectroscopy (DASH). Optics Express, 2010, 18, 27416.	1.7	43
54	The Aeronomy of Ice in the Mesosphere (AIM) mission: Overview and early science results. Journal of Atmospheric and Solar-Terrestrial Physics, 2009, 71, 289-299.	0.6	179

#	Article	IF	CITATIONS
55	High-altitude data assimilation system experiments for the northern summer mesosphere season of 2007. Journal of Atmospheric and Solar-Terrestrial Physics, 2009, 71, 531-551.	0.6	106
56	The diurnal variation of polar mesospheric cloud frequency near 55°N observed by SHIMMER. Journal of Atmospheric and Solar-Terrestrial Physics, 2009, 71, 401-407.	0.6	27
57	Spatial Heterodyne Imager for Chemicals and Atmospheric Detection (SHIMCAD): First Brassboard Results. , 2009, , .		Ο
58	Spatial Heterodyne Imager for Mesospheric Radicals (SHIMMER): Results from the First Satellite Borne SHS Spectrometer. , 2009, , .		1
59	The Doppler Asymmetric Spatial Heterodyne (DASH) Interferometer. , 2009, , .		1
60	First results from the Spatial Heterodyne Imager for Mesospheric Radicals (SHIMMER): Diurnal variation of mesospheric hydroxyl. Geophysical Research Letters, 2008, 35, .	1.5	24
61	Doppler asymmetric spatial heterodyne spectroscopy (DASH): concept and experimental demonstration. Applied Optics, 2007, 46, 7297.	2.1	92
62	Polar mesospheric cloud mass and the ice budget: 2. Application to satellite data sets. Journal of Geophysical Research, 2007, 112, .	3.3	20
63	Polar mesospheric cloud mass and the ice budget: 1. Quantitative interpretation of mid-UV cloud brightness observations. Journal of Geophysical Research, 2007, 112, .	3.3	11
64	SHIMCAD Breadboard: Design and Characterization Overview. , 2007, , .		0
65	Basic Principle of Doppler Asymmetric Spatial Heterodyne Spectroscopy (DASH): An Innovative Concept for Measuring Winds in Planetary Atmospheres. , 2007, , .		0
66	Flatfielding in spatial heterodyne spectroscopy. Applied Optics, 2006, 45, 4583.	2.1	56
67	Doppler asymmetric spatial heterodyne spectroscopy (DASH): an innovative concept for measuring winds in planetary atmospheres. , 2006, 6303, 272.		22
68	The polar mesospheric cloud mass in the Arctic summer. Journal of Geophysical Research, 2005, 110, .	3.3	31
69	Correction of Phase Distortion in Spatial Heterodyne Spectroscopy (SHS). , 2005, , .		0
70	Correction of phase distortion in spatial heterodyne spectroscopy. Applied Optics, 2004, 43, 6680.	2.1	56
71	Spatial Heterodyne Spectroscopy For High Spectral Resolution Space-Based Remote Sensing. Optics and Photonics News, 2004, 15, 46.	0.4	8
72	Robust monolithic ultraviolet interferometer for the SHIMMER instrument on STPSat-1. Applied Optics, 2003, 42, 2829.	2.1	56

#	Article	IF	CITATIONS
73	SHIMMER on STS-112: Development and Proof-of-Concept Flight. , 2003, , .		3
74	Polar mesospheric clouds formed from space shuttle exhaust. Geophysical Research Letters, 2003, 30, n/a-n/a.	1.5	62
75	Shimmer: a spatial heterodyne spectrometer for remote sensing of Earth' middle atmosphere. Applied Optics, 2002, 41, 1343.	2.1	90
76	OH observations of space shuttle exhaust. Geophysical Research Letters, 2002, 29, 16-1-16-4.	1.5	15
77	Discovery of a water vapor layer in the Arctic summer mesosphere: Implications for polar mesospheric clouds. Geophysical Research Letters, 2001, 28, 3601-3604.	1.5	63
78	PMCs and the water frost point in the Arctic summer mesosphere. Geophysical Research Letters, 2001, 28, 4449-4452.	1.5	28
79	THOMAS 2.5 THz measurements of middle atmospheric OH:Ccomparison with MAHRSI observations and model results. Geophysical Monograph Series, 2000, , 305-310.	0.1	2
80	The 2.5 THz heterodyne spectrometer THOMAS: Measurement of OH in the middle atmosphere and comparison with photochemical model results. Journal of Geophysical Research, 2000, 105, 22211-22223.	3.3	22
81	Photon induced far-infrared absorption in pure single crystal silicon. Infrared Physics and Technology, 1999, 40, 447-451.	1.3	7